Chin. J. Astron. Astrophys. Vol. 5 (2005), No. 4, 363–370
(*http://www.chjaa.org*)

Chinese Journal of
Astronomy and
Astrophysics

Evidence of Evolution in the Dense Cores in Massive Star Forming Regions *

Jian-Jun Zhou[1,2], Jarken Esimbek[1], Ji-Xian Sun[3], Bing-Gang Ju[3] and Jing-Jiang Sun[3]

[1] National Astronomical Observatories/Urumqi observatory, Chinese Academy of Sciences, Urumqi 830011; *zhoujj@ms.xjb.ac.cn*
[2] Graduate School of the Chinese Academy of Science, Beijing 100080
[3] Qinghai Station of Purple mountain Observatory, Chinese Academy of Science, Delingha, Qinghai 817000

Received 2004 December 6; accepted 2005 June 22

Abstract The excitation of H_2O masers usually needs very high density gas, hence it can serve as a marker of dense gas in HII region. We selected a sample of H_2O maser sources from Plume et al. (four with, and four without detected CS($J = 7 - 6$) emission), and observed them in ^{13}CO(J=1−0) and C^{18}O (J=1−0). C^{18}O (J=1−0) emission was detected only in three of the sources with detected CS(J=7−6) emission. An analysis combined with some data in the literature suggests that these dense cores may be located at different evolutionary stages. Multi-line observation study may provide us clues on the evolution of massive star forming regions and the massive stars themselves.

Key words: ISM: molecules – masers – radio lines: ISM–stars: formation

1 INTRODUCTION

Dense cores in molecular clouds ($n \geq 10^5$ cm^{-3}) are the sites of massive star formation, which determine the efficiency of star formation (Lada et al. 1991; Solomon, Radford & Downes 1990). However, the winds and radiation of newly formed stars can disrupt the local dense cloud cores and effectively shut down further star formation. On the other hand, very dense cloud cores can resist these disruptive forces and help to maintain star formation process (Plume et al. 1997). Thus a complete understanding of star forming activities in the Galaxy requires knowledge of the properties of molecular clouds where stars are forming. Detailed studies of some dense cores have yielded much information about the structure, excitation and chemistry, as well as the influence of the embedded stars (Carpenter et al. 1990; Plume et al. 1992, 1997; Hofner et al. 2000). C^{18}O and ^{13}CO are the best tracers of molecular gas with a density of $10^3 - 10^4$ cm^{-3} (Kato et al. 1999). C^{18}O is good at tracing the column density in the warm, dense gas of cluster forming regions and the overall structure of the warm gas pervading the cluster. C^{18}O

∗ Supported by the National Natural Science Foundation of China.

line shapes and velocities are good tracers of the gas kinematics and are relatively unaffected by the optical depth effects. ^{13}CO emission can be optically thick toward the cluster center, it thus traces the outer, more tenuous regions of the cluster, where C^{18}O is too weak to be mapped efficiently. These data therefore enable us to characterize the cluster-forming molecular gas from the regions of peak density toward the centers of each cluster out to the non-star-forming gas of the surrounding molecular cloud (Plume et al. 1997; Nagahama et al. 1998; Saito et al. 1999; Kato et al. 1999; Ridge et al. 2000).

H_2O masers are excited in extremely dense gas (Elitzur, Hollenbach & McKee 1989; Strelnitskij 1984), they can serve as a pointer of likely locations of dense gas (Plume et al. 1992, 1997). Plume et al. (1992) detected CS(J=7−6) emission in 104 out of 179 H_2O maser sources. It should be noted that CS(J=7−6) emission was not detected in some of the sources, maybe due to the poor signal to noise ratio (Plume et al. 1992). It might be safe for us to conclude that the CS(J=7−6) emission of these sources is very weak in any case. The critical density of CS(J=7−6) is about $\sim 2\times10^7$ cm^{-3}, so the physical and chemical state of the cloud cores with detected CS(J=7−6) emission may be different from those without the emission. We selected eight sources from Plume et al (1992) (four with detected CS(J=7−6) emission (Cep A, S255/7, IRAS 00338+6312 and W3(1)), four without (S266, S201, IRAS 03101+5821 and BFS44)), and made C^{18}O(J=1−0) and ^{13}CO(J=1−0) observations in their directions.

2 OBSERVATIONS

Our observations were made at the Qinghai station of PMO (Purple Mountain Observatory of China) from 2003 March 28 to April 10. The 14 m radio telescope worked in 85–115 GHz, with a pointing accuracy better than $10''$. The main beam width of the antenna is about $106''\times70''$, and the main beam efficiency is ∼42.12% at 112 GHz. The telescope is equipped with a 3 mm cooled SIS receiver with noise temperature about 60 K (DSB), and the system noise temperature at the zenith is 250 K (SSB). A 1024 channel AOS spectrometer has been installed on the terminal, the frequency resolution is 78.7 kHz (^{13}CO) and 75.7 kHz (C^{18}O). Our observations were made at 110.201 GHz (^{13}CO(J=1−0) and 109.782 GHz (C^{18}O (J=1−0)) in position-switching mode. We mapped a $6'\times6'$ region centered at the position of H_2O maser of each source with a grid spacing of $1'$. S255/7 is an exception, however, which was observed with a grid spacing of $30''$. The sensitivity of the system is 0.26 K(rms) for 1 minute integration time.

3 RESULTS

The data were reduced with the CLASS software package. The CO maps of the integrated intensity are presented in Fig. 1. Both C^{18}O(J=1−0) and ^{13}CO(J=1−0) emissions were detected toward S255/7, Cep A and IRAS 00338+6312. We plot C^{18}O in grey scale with ^{13}CO contours superimposed. We did not detect C^{18}O emission in W3(1), and four sources without CS(J=7−6) emission were detected. The ^{13}CO(J=1−0) maps of these five sources are plotted in contour levels. That C^{18}O emission was not detected in these five sources may not imply there is no C^{18}O emission. The system sensitivity of observations is 0.26 K(rms). This means if C^{18}O emission in these sources is weaker than 0.26 K, then we would not have detected it. Typical C^{18}O spectrum of these sources have an average rms of about 0.2 K (Fig. 2). Hence if there is C^{18}O emission in these sources, it must be weak. Keeping this in mind will help us to analyze the data and obtain correct conclusions.

Combined with the CO(J=1−0) data in the literature (Blitz, Fich & Stark 1982; Wouterloot & Brand 1989), we calculated the column density of ^{13}CO using the formula

$$N(^{13}\mathrm{CO}) = 2.13\times10^{14}\frac{\int T_R^*(^{13}\mathrm{CO})dv}{1-\exp(5.29/T_{\mathrm{ex}})}(\mathrm{cm}^{-2})\,,$$

Table 1 Parameters of all eight sources. Here $\int T_R^* dv$ and Δv are the corresponding values of ^{13}CO(J=1−0). N is the column density of ^{13}CO in the maser site. The total infrared luminosity of the star associated with the H_2O maser (L) and distance (Dis) are cited from Wouterloot & Brand (1989) and Palagi et al (1993). Δv_{2-1} and Δv_{3-2} denote the FWHM of CS(J=2−1) and CS(J=3−2) cited from Plume et al. (1997).

Source	R.A. α (J2000)	Decl δ (J2000)	$\int T_R^* dv$ K km s^{-1}	Δv km s^{-1}	N cm^{-2}	L $L_\odot$	Dis kpc	Δv_{2-1} km s^{-1}	Δv_{3-2} km s^{-1}
Cep A	22:56:17.932	+62:01:49.345	26.78	2.77	2.69E16	7.4E4	1.4	4.7	5.4
S255/7	06:12:53.617	+17:59:27.037	35.23	3.50	4.75E16	2.8E4	1.65	3.1	4
IRAS-00338+6312	00:36:47.509	+63:29:02.077	5.94	1.71	5.17E15	3.0E3	1.61	4.5	5.1
W3 (1)	02:25:28.226	+62:06:57.678	4.54	2.77	4.76E15		3.18	3.3	4.3
S266	06:17:24.297	+14:54:37.206	3.85	2.59	2.46E15	1.5E4	12.83	2.7	2.2
S201	03:03:19.684	+60:27:56.287	1.75	2.50	1.45E15	2.5E4	3.96	2	3.5
IRAS-03101+5821	03:14:06.384	+58:33:09.837	2.09	1.21	1.60E15	1.4E3	4.04	1.9	2.8
BFS44	04:51:38.678	+45:35:33.028	1.10	0.12	5.12E14	1.8E3	4.83		

on the assumption of local thermodynamic equilibrium (Nagahama et al. 1998). We obtained integrated intensity ($\int T_R^* dv$) and full width at half maximum (FWHM) (Δv) by Gaussian fit (see Table 1). Here column 1 gives the source name, columns 2 and 3, the equatorial coordinates of the maser site. $\int T_R^*(^{13}\mathrm{CO}) dv$, Δv (^{13}CO) and N(^{13}CO) are listed in columns 4, 5, and 6, respectively. The total infrared luminosity of the infrared source associated with the H_2O masers and the corresponding distance are given in columns 7 and 8 (Wouterloot & Brand 1989; Palagi et al. 1993). Columns 9 and 10 list the FWHM of CS(J=2−1) and CS(J=3−2) (Plume et al. 1997).

A brief description of each source and our CO map now follow.

Cep A: Cepheus A is a famous star forming region, and has been studied by many authors (Blitz & Lada 1979; Beichman, Becklin & Wynn-Williams 1979; Rodriguez, Ho & Moran 1980). IRAS 22543+6415 is associated with the H_2O masers at an offset $\Delta\alpha$=8.6″, $\Delta\delta$=10.9″ (Palagi et al. 1993). The $C^{18}O$ emission is relatively weak (see Fig. 1). There are some holes and two weak $C^{18}O$ emission peaks in the map. The ^{13}CO emission is weak in the north of the H_2O maser site, but becomes stronger towards the south. The ^{13}CO emission peak is coincident with a $C^{18}O$ peak lying in the southeast of the H_2O maser site.

S255/7: S255 and S257 are members of a cluster of optically visible HII regions S254–258. There is an embedded star formation complex between S255 and S257, which contains far infrared sources, UC HII regions and molecular outflows (Snell & Bally 1986; Kurtz, Churchwell & Wood 1994; Miralles et al. 1997). The infrared source associated with the H_2O maser is IRAS 06099+1800, which is located to the southwest of the H_2O maser site at an offset $\Delta\alpha = -4.3''$, $\Delta\delta = -5.0''$ (Palagi et al. 1993). Our observations show that the $C^{18}O$ emission is weaker than that of ^{13}CO (see Fig. 1). Two weak $C^{18}O$ emission peaks located to the east and northeast of the H_2O maser site, which are coincident with the ^{13}CO emission peak. The distribution of ^{13}CO emission is relatively smooth.

IRAS 00338+6312: This is a young stellar object located near the core of dark cloud L1287, driving a strong molecular outflow (Yang et al. 1991; David et al. 1993). The cloud mass associated with it is in the range from $2.2 \times 10^3 M_\odot$ to $2.7 \times 10^3 M_\odot$ (Carpenter, Snell &

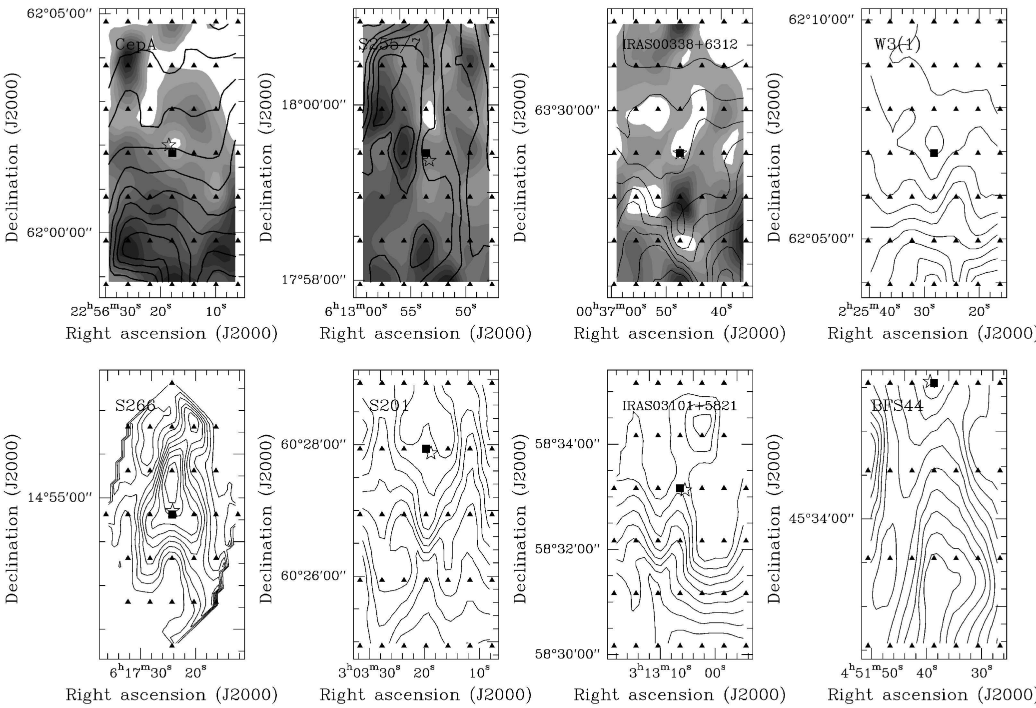

Fig. 1 Integrated intensity CO maps of eight sources. We plot $C^{18}O(J{=}1-0)$ in grey scale and $^{13}CO(J{=}1-0)$ in contour lines. The peak values of ^{12}CO of these sources are 62.921, 53.784, 26.646, 48.844, 4.778, 12.557, 12.636 and 7.795 K km s^{-1}, the contour levels are at 90%, 80%, ..., 10% of the peak. The ^{13}CO peaks of Cep A, S255/7 and IRAS 00338+6312 are 9.912, 6.888 and 5.882 K km s^{-1}, respectively. Here the filled rectangle denotes the H_2O maser site, and the open pentagon denotes infrared sources associated with them.

Schloerb 1990). The H_2O maser is coincident with that of IRAS 00338+6312 (Palagi et al. 1993). $C^{18}O$ emission is weak (see Fig. 1). There are some big cavities in the $C^{18}O$ map, and one weak peak lies to the south of the H_2O maser site. ^{13}CO emission is weak in the north of H_2O maser site, but it becomes stronger with decreasing declination. There is no ^{13}CO emission peak in the map.

W3 (1): W3 complex consists of a giant molecular cloud with numerous HII regions and luminous infrared sources. It has been studied in the near and far infrared (Wynn-Williams et al. 1972; Werner et al. 1980), in molecular lines (Claussen et al. 1984; Thronson 1986; Helmich et al. 1994) and in radio wavelengths (Roelfsema et al. 1987). This H_2O maser has no associated infrared source (Palagi et al. 1993). ^{13}CO emission was quite weak in the north of the H_2O maser site, but it becomes stronger with decreasing declination. It seems there is a ^{13}CO emission peak near the bottom of map.

S266: The nebulae, S266, was discovered by Sharpless (1959). Recent narrow-band H_α image and high resolution spectroscopy of S266 indicate that its central star, MWC137, is a supergiant Be star, and S266 is a ring nebula around this star (Esteban 1998). The H_2O maser is associated

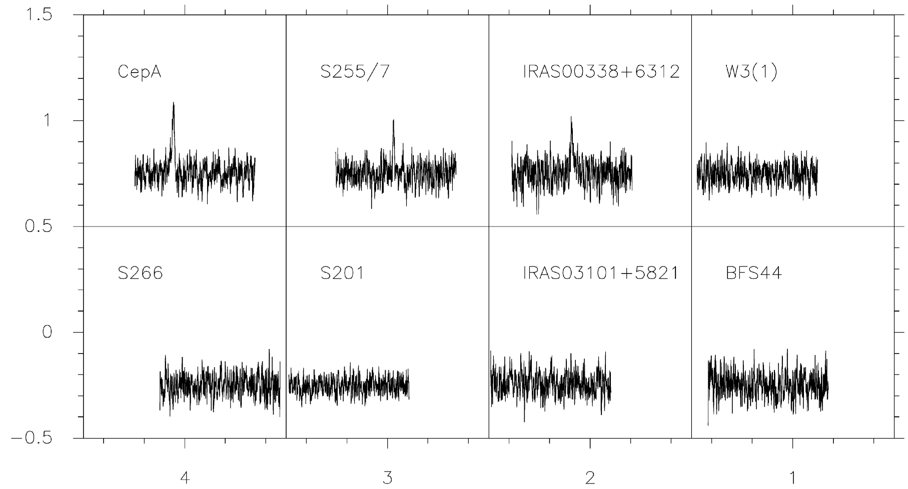

Fig. 2 Typical $C^{18}O$ ($J = 1 - 0$) spectrum of eight sources. Their rms values are 0.198 K, 0.189 K, 0.22 K, 0.207 K, 0.219 K, 0.153 K, 0.212 K and 0.22 K, respectively.

with IRAS 06145+1455, with an offset $\Delta\alpha = 1.5''$ and $\Delta\delta = -5.0''$(Palagi et al. 1993). ^{13}CO emission concentrates in a small area around the maser site, and ^{13}CO emission peaks at the north of H_2O maser site. Irregular morphology of ^{13}CO clump indicates that CO gas may be interacted with the ambient interstellar medium.

S201: S201 is apparently the eastern-most member of the string of HII regions dominated by the giants W3, W4 and W5 (Martin & Barrett 1978; Lada et al. 1978). It coincides with IRAS 02593+6016 and appears on the POSS plate as a nebula with an obscuring lane running through it. IRAS 02593+6016 is located to the southwest of the H_2O maser site at an offset $\Delta\alpha = -13.4''$and $\Delta\delta = -4.0''$ (Palagi et al. 1993). The ^{13}CO emission is weak in the north of the map, but it becomes stronger with decreasing declination (see Fig. 1). It seems there is a big cavity around the infrared star and the H_2O maser site in the ^{13}CO map.

IRAS 03101+5821: It is located in an active star-forming region. IRAS 03101+5821 is the target of many surveys (Wouterloot & Brand 1989; Palumbo et al. 1994; Nyman & May 1995), but it has not been studied in detail. H_2O maser associated with IRAS 03101+5821 was detected by Comoretto et al. (1990), which is located to the northeast of infrared star with an offset $\Delta\alpha$=13.4$''$ and $\Delta\delta$=2.1$''$ (Palagi et al. 1993). There is little ^{13}CO emission in the north of maser site. ^{13}CO emission becomes stronger to the south of the maser site. No ^{13}CO emission peak appears in the map.

BFS44: It is an optically visible Galactic HII region, and is associated with a molecular cloud complex and various masers. BFS44 has been observed in several surveys (Wouterloot & Brand 1989; Koo, Heiles & Reach 1992; Palagi et al. 1993). The infrared source, IRAS 04480+4530, is located at northeast of H_2O maser site with an offset $\Delta\alpha$=10.5$''$ and $\Delta\delta$=1.0$''$(Palagi et al. 1993). ^{13}CO emission was detected only in the south of H_2O maser site. ^{13}CO emission becomes stronger with the decrease of declination, and there is a ^{13}CO emission peak in the south of H_2O maser site.

4 DISCUSSION

Both CS(J=3−2) and CS(J=2−1) emissions were detected to all eight sources (Plume et al. 1997). This means that these dense cloud cores associated with H_2O masers are rich in intermediate density gas. $C^{18}O$ and ^{13}CO are effective in tracing the outer, tenuous gas of the dense clumps. However, no $C^{18}O$ emission was detected in the sources W3(1), S266, S201, IRAS 03101+5821 and BFS44. Because the system sensitivity of our observation is about 0.2 K (Fig. 2), if there is $C^{18}O$ emission in these five sources, it must be weak. There are some structures such as holes and cavities in the $C^{18}O$ map of Cep A, S255/7 and IRAS 00338+6312. All eight sources show a relatively smooth distribution of the ^{13}CO.

We notice that massive stars are formed in the dense cores of giant molecular clouds, and evolution of the central star will influence the natal cloud cores. Its strong wind and radiation will create an HII region and finally disrupt the natal cores. So the molecular environments of star forming region have been changing all the time. For four sources with detected CS (J=7−6) emission, three show both $C^{18}O$ and ^{13}CO emissions, while four show only ^{13}CO emission. One possible reason is the variation of the abundance ratio of ^{13}CO to $C^{18}O$. Though the dense cloud cores associated with H_2O masers are usually not coincident with associated infrared sources, they are affected by the strong wind and radiation of the newly formed star. The star will illuminate the outer, tenuous gas of the dense clumps and determine its physical and chemical properties. Self-shielding hence plays an important role in the dissociation and formation of CO. Because the self-shielding of ^{13}CO is much more efficient than that of $C^{18}O$, if the extinction is low and FUV radiation field is strong in the region, ^{13}CO will be enriched and $C^{18}O$ will become depleted due to dissociation (Strörzer et al. 2000). On the other hand, the abundance ratio of $^{13}CO/C^{18}O$ may keep constant and the outer part of the dense cloud cores may become tenuous. When ^{13}CO emission is just detectable, we cannot expect to detect $C^{18}O$ due to its low abundance. In fact, the column densities are higher in the four sources with detected CS(J=7−6) emission than in the other four sources (Table 1). Of course, this will make it easier for the $C^{18}O$ to be dissociated too. It is probable that variations in the $^{13}CO/C^{18}O$ ratio and in the gas density both play a role in determining the emission of ^{13}CO and $C^{18}O$.

Figure 3 shows the corresponding correlations of some parameters, and all of them refer to the H_2O maser sites. We see that $\log N(^{13}CO)$-FWHM ($^{13}CO(J{=}1{-}0)$) and $\log N(^{13}CO)$-$\int T_R^* dv$ show a good correlation, which is consistent with the theory of molecular line emission. The FWHM of ^{13}CO lines correlates very well with the infrared luminosity of the associated star. This implies that the infrared radiation of the star heat the outer, tenuous gas of dense cores, and the FWHM mainly reflects the thermal motion of the gas. The excitation of CS(J=2−1) emission needs higher density, so CS(J=2−1) emission should originate deeper inside the cores, and its physical and chemical state are not strongly influenced by the star. This may be the reason that the FWHM of CS(J=2−1) does not correlate with the infrared luminosity of the star. The FWHM of CS (J=2−1) and that of ^{13}CO show no correlations, this further supports the view that ^{13}CO and CS(J=2−1) emissions originate at different depths in the cloud cores and are dominated by different conditions. The FWHM of CS(J=2−1) correlates well with the CS(J=3−2), indicating that they originate in the same regions of the cloud cores and are dominated by the same conditions. The column densities of those without detected CS(J=7−6) emission have relatively much more tenuous gas (Table 1). The outer gas of these dense cores may have been dissipated or depleted by the strong wind and radiation of the newly formed star during its evolution. There was little $C^{18}O(J{=}1{-}0)$ in this tenuous gas, hence we cannot expect to detect it. The mean column density of CS is higher in the sources with detected CS(J=7−6) emission than in the sources without (Plume et al. 1997). Hence we think that the dense cloud cores with detected CS(J=7−6) emission are apparently in a relatively earlier phase than the other sources, and that they are not seriously affected by the young stars. That many different molecular line emission originate from different depths of the dense cores provides us an opportunity to study their physical and chemical state and evolution stage. A detailed study of the molecular environments of the HII regions may give us information on the evolution of massive stars.

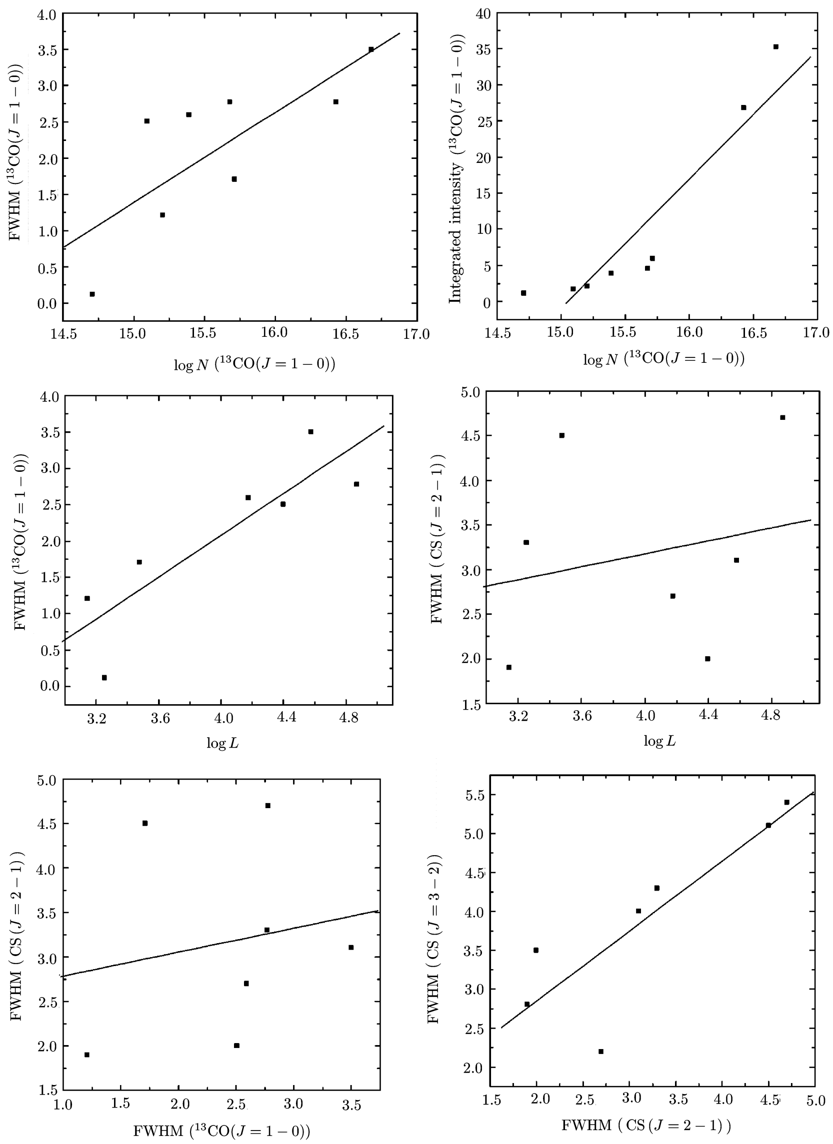

Fig. 3 Correlations of some parameters (see Table 1).

5 CONCLUSIONS

The rapid evolution of a massive star will interact strongly with its ambient cloud and influence its physical and chemical state, so multi-line study of dense cloud cores may provide us clues on the process of formation of massive stars. Our ^{13}CO and $C^{18}O$ observations toward eight dense cloud cores associated with H_2O masers, combined with the CS data from Plume et al. (1992, 1997), indicate that these dense cloud cores may be located in different evolutionary stages. We cannot determine the evolutionary sequence of the corresponding HII regions because of lack of data. However, it seems feasible to obtain the information of the evolution of HII regions and massive stars by examining the physical and chemical conditions of their molecular environments.

Acknowledgements This work was supported by the National Natural Science Foundation of China through Grant 10203003.

References

Beichman C. A., Becklin E. E., Wynn-Williams C. G., 1979, ApJ, 232, L47
Blitz L., Lada C. J., 1979, ApJ, 227, 152
Brofman L., Nyman L. -A., May J. 1995, A&AS, 115, 81
Carpenter J. M., Snell R. L., Schloerb F. P., 1990, ApJ, 362, 147
Claussen M. J., Berge G. L., Heiligman G. M. et al., 1984, ApJ, 285, L79
Comoretto G., Palagi F., Cesaroni R. et al. 1990, A&AS, 84, 179
Weintraub David A., Kastner J., 1993, ApJ, 411, 767
Elitzur M., Hollenbach D. J., McKee C. F., 1989, ApJ, 346, 983
Esteban C., 1998, MNRAS, 298, 185
Helmich F. P., Jansen D. J., de Graauw Th. et al., 1994, A&A, 283, 626
Hofner P., Wyrowski F., Walmsley C. M. et al., 2000, ApJ, 536, 393
Kato S., Mizuno N., Asayama S. et al., 1999, PASJ, 51, 883
Koo Bon-Chui Heiles C., Reach W. T., 1992, ApJ, 390, 108
Kurtz S., Churchwell E., Wood D. O. S., 1994, ApJS, 91, 659
Lada C. J., Depoy D. L., Merrill K. M. et al., 1991, ApJ, 374, 533
Lada C. J., Elmegreen B. G., Cong H. et al., 1978, ApJ, 226, L39
Martin R. N., and Barrett A. H., 1978, ApJS, 36, 1
Miralles M. P., Salas L., Cruz-Gonzalez I., Kurtz S., 1997, ApJ, 488, 749
Nagahama T., Mizuno A., Ogawa H. et al., 1998, AJ, 116, 336
Palagi F., Cesaroni R., Comoretto G. et al., 1993, A&AS, 101, 153
Palumbo G. G. C., Scappini F., Pareschi G. et al., 1994, MNRAS, 266, 123
Plume R., Jaffe D. T., Evans II N. J., 1992, ApJS, 78, 505
Plume R., Jaffe D. T., Evans II N. J., 1997, ApJ, 476, 730
Rodriguez L. F., Moran J. M., Ho P. T. P., 1980, ApJ, 240, L149
Roelfsema P. R., Goss W. M., Wilson T. L., 1987, A&A, 174, 232
Saito M., Kitamura Y., Kawabe R. et al., 1999, Proceedings of Star Formation 1999, Held in Nagoya, Japan, June 21-25, 1999, Editor: T. Nakamoto, Nobeyama Radio Observatory, p.207
Sharpless S., 1959, ApJS, 4, 257
Snell R. L., Bally J., 1986, ApJ, 303, 683
Solomon P. M., Radford S. J. E., Downes D., 1990, ApJ, 348, L53
Strörzer H., Zielinsky M., Stutzki J. et al., 2000, A&A, 358,433
Strelnitskij V. S., 1984, MNRAS, 207, 339
Thronson H. A., 1986, ApJ, 306, 160
Werner M. W., Becklin E. E., Gatley I., 1980, ApJ, 242, 601
Wouterloot J. G. A., Brand J., 1989, A&AS, 80, 149
Wramdemark S., Lynga G., 1987, in Star Forming Regions, IAU Symp., 115, eds. M. Peimbert, J. Jugaku, Reidel, Dordrecht, p.211
Wynn-Williams C. G., Becklin E. E., Neugebauer G., 1972, MNRAS, 160, 1
Yang J., Umemoto T., Iwata T. et al., 1991, ApJ, 373, 137
Zielinsky M., Stutzki J., Strörzer H., 2003, A&A, 358, 723